GEODYNAMICS & TECTONOPHYSICS
Published by the Institute of the Earth's Crust, Siberian Branch, Russian Academy of Sciences
PALEOGEODYNAMICS

2024 VOLUME 15 ISSUE 3 ARTICLE 0757 ISSN 2078-502X

DOI: 10.5800/GT-2024-15-3-0757

THE SHALAP MÉLANGE OF THE SALAIRIAN ALAMBAY OPHIOLITE ZONE (NORTHWESTERN CENTRAL ASIAN OROGENIC BELT), GEOLOGICAL STRUCTURE AND COMPOSITIONAL FEATURES OF AMPHIBOLITES AND GREENSTONE BASALTS

F.I. Zhimulev [1✉], **A.V. Kotlyarov** [1], **A.V. Travin** [1,2], **M.A. Fidler** [1], **A.A. Khuurak** [1]

[1] Sobolev Institute of Geology and Mineralogy, Siberian Branch of the Russian Academy of Sciences, 3 Academician Koptyug Ave, Novosibirsk 630090, Russia
[2] Novosibirsk State Technical University, 20-1 Karl Marx Ave, Novosibirsk 630073, Russia

ABSTRACT. The Alambay ophiolite zone (AOZ) is located in the axial part of the Early Paleozoic Salairian orogen and includes the northern extension of the Alambay-Kaim zone, Salair and Altai Mountains. The Shalap area of the AOZ is predominantly composed of clastic mélange with occasional serpentine mélange. The geological and geochemical studies showed that in the Shalap mélange there are basalt blocks of the Alambay formation whose petrogeochemical features are similar to those of the oceanic island basalts (OIB). Metamorphic rocks of the Angurep complex, represented by garnet and non-garnet amphibolites, form a tectonic slab which is a part of the accretionary complex east of the Shalap mélange area. Metamorphic rocks also form blocks in the Shalap mélange. The amphibolites of the Angurep complex are similar in their petrogeochemical features to the basalts of intraoceanic island arcs. The Shalap mélange is a fragment of the Salairian Cambrian paleosubduction zone. The subduction and exhumation processes in this paleosubduction zone terminated by the 500 Ma time stage.

KEYWORDS: amphibolites; basalts; subduction mélange; accretionary complex; ophiolites

FUNDING: The research was supported by the Russian Science Foundation (project 23-27-00033).

EDN: LSFJDC

RESEARCH ARTICLE

Received: April 10, 2023
Revised: August 7, 2023
Accepted: August 14, 2023

Correspondence: Fedor I. Zhimulev, zhimulev@igm.nsc.ru

FOR CITATION: Zhimulev F.I., Kotlyarov A.V., Travin A.V., Fidler M.A., Khuurak A.A., 2024. The Shalap Mélange of the Salairian Alambay Ophiolite Zone (Northwestern Central Asian Orogenic Belt), Geological Structure and Compositional Features of Amphibolites and Greenstone Basalts. Geodynamics & Tectonophysics 15 (3), 0757. doi:10.5800/GT-2024-15-3-0757

1. INTRODUCTION

The ophiolite zones yield clues about the oceanic basins of the past. The information about their-contained evolving oceanic basins approximately several thousand km long and geological processes in the subduction zone is constrained to a narrow band of subduction-related mélange. Geochemical features of basalts and basaltic rocks from mélange can be used to determine tectonic conditions for the formation of the oceanic crust. The Alambay ophiolite zone (AOZ) is one of the ophiolite stuctures of the Altai-Sayan Folded Area (ASFA) of the Central Asian Orogenic Belt (CAOB) to which modern research methods were least applied [Konovalova, Prusevich, 1977; Pinus et al., 1958]. It is located in an axial part of the Early Paleozoic Salairian fold-nappe structure (orogen) and includes the northern extension of the Alambay-Kaim zone, Salair, and Altai Mountains [Shokalskii et al., 2000]. The AOZ contains several en echelon lens-shaped areas. The northwestern, Tyagun-Alambay area is confined to the middle part of the Salair. The southeastern, Shalap (Martynovo-Shalap) area, forms an axial part of the southwestern flank of the Salair (Fig. 1). The Shalap area is predominantly composed of terrigenous mélange with occasional serpentinite mélange. The aim of this study is to make assumptions about formation conditions of the Shalap ophiolite mélange based on the characteristics of the geological structure and composition of metabasites therefrom.

2. GEOLOGICAL STRUCTURE OF THE SHALAP MÉLANGE

Within the ophiolite zone, there are distinguished the Alambay basalt, upper Alambay dunite-harzburgite and Shalap mélange geological complexes. Besides, the AOZ is structurally associated with a tectonic slab of amphibolites recognized as the Angurep metamorphic complex [Shokalskii et al., 2000; State Geological Map..., 2019]. The

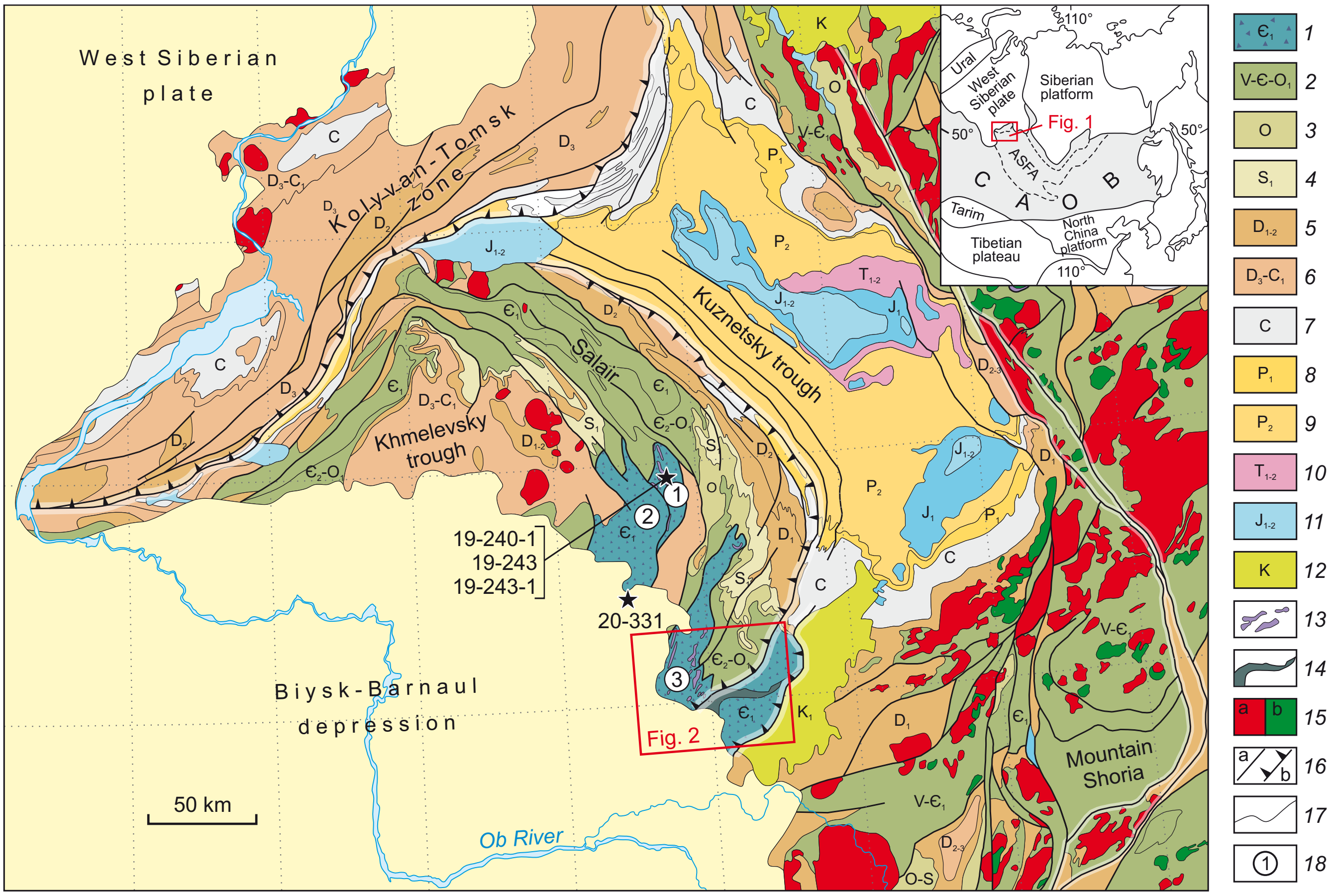

Fig. 1. Geological map of the Salair Ridge (after [State Geological Map..., 2007]).
1–2 – Vendian (?) – Early Ordovician folded basement: *1* – subduction mélange of the Alambay ophiolite zone, including basalts, shists, limestones, and serpentinites, *2* – paleoisland-arc complexes undissected; *3–6* – deformed Paleozoic sedimentary cover: *3* – carbonate-clastic Ordovician, *4* – carbonate-clastic Silurian, *5* – volcanic Devonian, *6* – clastic Upper Devonian and Lower Carboniferous; *7–9* – sedimentary infill of the Late Paleozoic troughs: *7* – clastic Carboniferous, *8* – coal-bearing Lower Permian, *9* – non-coal clastic Upper Permian; *10* – Triassic plateaubasalts; *11* – Lower–Middle Jurassic clastic coal-bearing deposits of the superimposed basins; *12* – Lower Cretaceous, shales and sandstones; *13* – bodies of ultramafic rocks; *14* – amphibolite layer of the Angurep complex; *15* – granitoid intrusions (a), diorite-gabbro intrusions (b); *16* – faults (a), frontal thrusts of the Salair and Kolyvan-Tomsk folded zone (b); *17* – stratigraphic boundaries; *18* – subduction mélange areas: 1 – Tyagun-Alambay, 2 – Kytmanov, 3 – Shalap. The asterisks indicate the positions of the samples taken beyond Fig. 2, from the Kytmanov and Togul-Sungai subduction mélange areas (App. 1, Table 1.1).

Shalap mélange complex as a mapped tectonic-stratigraphic subdivision was identified by V.N. Tokarev during cartographic mapping [State Geological Map..., 2019]. In view of the presence of the Devonian lens-shaped tectonic blocks in the mélange area field, V.N. Tokarev considered the Shalap mélange as tectonic, formed in the Permian in result of thrusting Salair slab of allochthonous material over the Kuzbass along the imbricated zone. From our point of view, the Shalap area represents the Cambrian subduction mélange, which underwent the Late Paleozoic thrust deformations as well as all the Salair orogenic formations did, so that the Devonian tectonic sediment slabs occurring in the mélange field, unlike microquartzite, limestone, serpentinite and amphibolite blocks, are not syngenetic inclusions of the ophiolite mélange. This is supported by the composition of terrigenous mélange matrix, represented by common sedimentary rocks with different degrees of tectonic reworking, the composition of blocks-inclusions in mélange, and a number of geological features which allow the Shalap mélange to be related to the category of subduction mélanges [Festa et al., 2010; Raymond, 2019]. The mélange complex has a widespread occurrence in the southern Alambay ophiolite zone, within the Shalap area (Fig. 2). It is traced as a band up to 22 km wide and about 120 km long. The band has an inhomogeneous structure and includes lens-shaped serpentinite and terrigenous mélange bodies.

According to the geophysical data, the depth distribution of mélange exceeds 5–6 km. Serpentinite mélange is studied in well core to a depth of 500 m; it is represented by serpentinite schists with several-kilometer massive serpentinized dunite and harzburgite blocks. Terrigenous mélange comprises a major part of the complex. The lumps and blocks of mélange are composed of amphibolites from the Angurep metamorphic complex, high-Ti basalts from the Alambay formation, siliceous schists and microquartzites (Fig. 3, a–c), and marbleized limestones of the Gavrilov formation, Lower Cambrian [State Geological Map..., 2019]. The terrigenous mélange matrix has non-uniform composition represented by aleurolites and volcanomictic greywacke sandstones admixed with carbonates, siliceous material, ore dust and carbonaceous matter. Mélange is

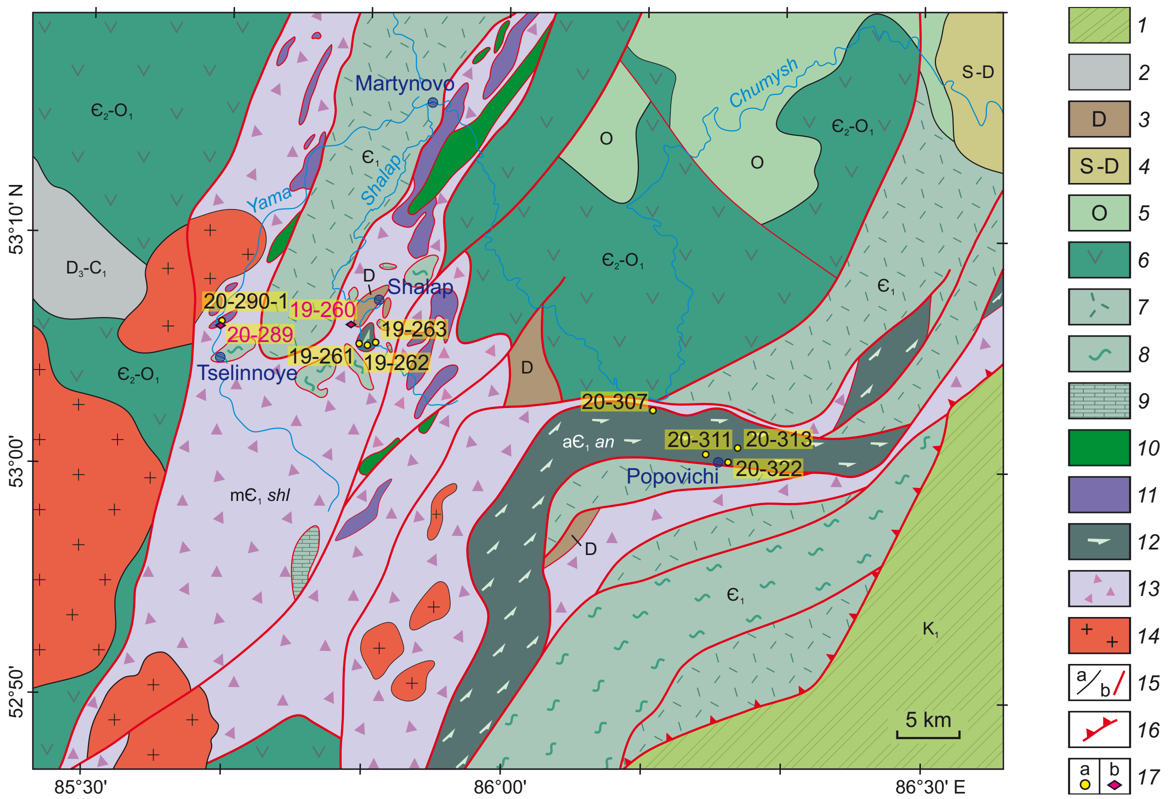

Fig. 2. Geological map of the Shalap area of the AOZ with sampling sites (after [Dobretsov et al., 2004; State Geological Map..., 2019; Zhimulev et al., 2023]).

1 – Lower Cretaceous deposits of the Nenya-Chumysh basin; *2–5* – deformed fragments of the Salair cover: *2* – Upper Devonian – Lower Carboniferous sandstones and siltstones of the Khmelevsky trough, *3* – Devonian limestones and sandstones, *4* – Silurian-Devonian limestones and sandstones, *5* – Ordovician sandstones; *6* – Middle Cambrian – Lower Ordovician tuffs, lavas and sandstones of island-arc origin; *7* – Vendian – Lower Cambrian tuffs, lavas and sandstones of island-arc origin; *8* – Vendian-Lower Cambrian carbonaceous shales, siltstones, microquartzites and limestones (sedimentary part of the ophiolite section and carbonate cap of the paleoisland); *9* – Lower Cambrian limestone block mélanges; *10* – ophiolite gabbro; *11* – serpentinized ultramafic rocks; *12* – Early Cambrian amphibolites of the Angurep metamorphic complex; *13* – Shalap polymictic subduction mélange; *14* – undissected granites (Ordovician (?), Late Devonian, Late Permian); *15* – geological boundaries: a – stratigraphic and intrusive, b – tectonic; *16* – Barka thrust, southern border of Salair; *17* – sampling sites and numbers of selected samples (a), photo of outcrops (b).

intruded by the Late Permian plagiogranites of the Zhernov complex with a U-Pb zircon age of 262.2±2.3 Ma [State Geological Map..., 2019]. Most of the outcrops of the Shalap mélange represent microquartzite and clay-rich siliceous shale blocks (Fig. 3, a), containing, among other things, manganese oxide mineralization (Fig. 3, b). The microquartzite blocks vary in size from a few meters to a few hundreds of meters. The microquartzite blocks form chains elongated parallel to the structures commonly striking northeast. Microquartzites comprise a range of hills near Tselinnoye settlement. The microquartzite blocks lie in the matrix materials made up of greenish-gray aleuritic greywackes with different degrees of tectonization. Near Tselinnoye and Shalap settlements, there is a large proportion

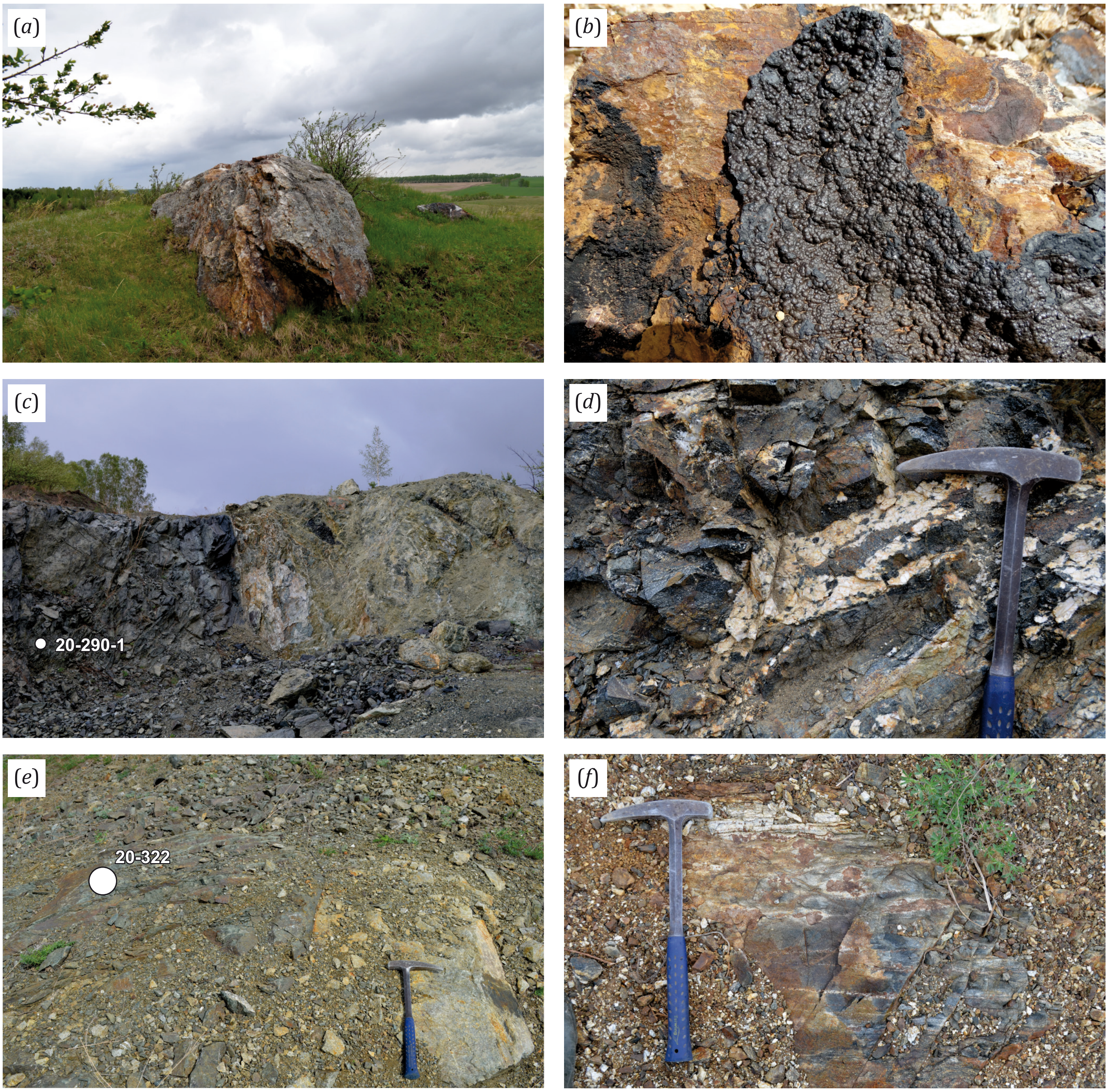

Fig. 3. Photographs of outcrops of the Shalap mélange and the Angurep metamorphic complex.
(*a*) – Shalap microquartzite block mélange (observation point (OP) 20-289, 53°6′4.22" N, 85°39'25.72" E); (*b*) – sinter aggregates of manganese hydroxide in the weathering crust along the aggregation pathways of manganese quartzites and siliceous mudstones forming the Shalap block mélange (OP 19-260, 53°6'12.48" N, 85°48'49.05" E); (*c*) – greenstone basalt block (left) in serpentinite mélange, sampling site 20-290-1 (53°6'16.62" N, 85°39'31.74" E); (*d*) – migmatite veinlets in amphibolites of the Angurep complex, sampling site 20-307 (53°2'49.38" N, 86°10'25.22" E); (*e*) – microplagiogranite dike (right) cutting through the amphibolites of the Angurep complex, sampling site 20-322 (53°0'12.61" N, 86°15'46.28" E); (*f*) – deformed garnet glomeroblasts in migmatized amphibolites (OP 20-330, 52°57'14.03" N, 85°27'51.94" E).

of microquartzite blocks in terrigenous mélange, with the matrix rock strongly tectonized up to the formation of folded schists. To the east, along the Yama River valley, there is a decrease in the proportion of rock inclusions in mélange and in the degree of tectonic reworking of matrix rock, so that mélange gradually re-forms into common sedimentary rock composed of fine-grained greywackes. Eastward of the Shalap area, there are some more mélange lenses and bands of smaller size. The tectonic slabs of volcanites, flysches and limestones are intercalated within the mélange zone. On the magnetotelluric (MTS) profile, intersecting the southern Salair structures, the mélange area represents the conduct anomaly with an inhomogeneous inner structure [Zhimulev et al., 2023]. The profile shows that the block with relatively high electrical resistivity, corresponding to the tectonic slab of metamorphic rock of the Angurep complex, is located within the conduction area composed of the Shalap area complexes of the AOZ. The slab of rock of the Angurep complex can be considered as a part of structural-substantial paragenesis of the paleosubduction zone.

3. ANGUREP METAMORPHIC COMPLEX

Garnet amphibolites of the Angurep metamorphic complex eastward of the Shalap mélange area comprise a 2–4 km thick tectonic slab that can be traced in rare outcrops over a distance of about 60 km in accordance with the geophysical data. The slab has a sublatitudinal strike in the northern part and a submeridional strike in the southwestern part. Metamorphic rocks in geophysical fields are accompanied by positive gravity anomalies. On the north and northwest, the tectonic slab of metamorphic rocks is superimposed with a slab of the Lower Cambrian volcanites, on the south and southeast – with a stratum comprising a wide range of materials such as volcanomictic sandstones, conglomerates, limestones and volcanites, interpreted as an olistostrome in the accretionary wedge [Dobretsov et al., 2004]. The fault zones, bordering a slab of metamorphic rocks, are traced by foliated serpentinite and graphitic milonite bodies.

Metamorphic rocks are represented by garnet-bearing and non-garnet amphibolites; the cross-section exhibits both fine- and coarse-grained varieties (Fig. 3, d–f). Plagioclase in amphibolites has partly saussuritized (Fig. 4). Amphibolites in some areas are intensely migmatized. Numerous granitoid segregations in a stratum of amphibolite are of two morphological types: 1) conformable striation directions, twisted veinlets, irregularly shaped lenses and segregations with twisted contacts (see Fig. 3, d), 2) dikes with smooth intrusive contacts intersecting banded amphibolites (see Fig. 3, e). According to S.A. Kargopolov's data on amphibolite mineral chemistry [Vladimirov et al., 1994], three types of rocks can be distinguished based on the composition of coexisting garnets within the garnet-bearing unit: 1) with high-magnesial garnet (Prp>20–30 %), 2) with grossular-almandine (Prp – 10–15 %), 3) with manganous glossular-almandine (Prp<10 %). The highest Mg garnet samples also show the highest aluminum concentrations in amphiboles (up to 17 wt. % of $Al_2 0_3$). Such amphiboles have low alkaline and Ti contents and belong to the actinolite-chermakite group. The Mg garnet samples include rutile; the association of magnesian garnet, aluminiferous amphibole and rutile is considered as a high-pressure metamorphism product. A widespread occurrence of migmatites and granitiod veins in a stratum of amphibolites is indicative of the partial melting during metamorphism. In accordance with S.A. Kargopolov's estimates, the thermodynamic parameters of metamorphic amphibolites both from the Angurep slab and Shalap mélange are 600–650 °C and 8–9 kbar [Vladimirov et al., 1994; Zhimulev et al., 2020]. The age of metamorphic amphiboles from the Angurep complex was determined by A.V. Travin and S.A. Kargopolov through $^{40}Ar/^{39}Ar$ isotopic dating of chermakite amphibole from the garnet-bearing amphibolite sample. High-pressure paragenesis revealed from this sample includes Qz+Pl+Hbl1+Grt+Rt. Secondary minerals are presented by Ep+Ms+Chl+Hbl2 association. Secondary amphibole (Hbl2) occurs rarely as actinolitic hornblende and actinolite. Dating was performed on a monofraction of chermakite amphibole, typical of high-pressure paragenesis. On the age spectrum diagram of the sample there is a plateau characterized by 520±2 Ma and a 60 % share of released ^{39}Ar [Vladimirov et al., 1994; Zhimulev et al., 2020]. The closure temperature of K/Ar isotopic system of amphibole (500–550 °C) is lower than the temperature of the described mineral paragenesis, so that the obtained value can be considered as the upper age limit for peak metamorphism.

4. GEOLOGICAL SETTING OF THE SELECTED SAMPLING AREAS

In the Shalap mélange distribution field there were selected samples 19-261, 19-262, 19-263, and 20-290-1 (see Fig. 2). A more than 10-m lens of serpentinite mélange with a greenstone aphyric basalt block was penetrated in the Yama River valley slope (see Fig. 3, c; Fig. 4). Greenstone basalts are composed of plagioclase microcrystals plunged into the matrix of chloritized volcanic glass. The rock is cataclastic. A block of garnet-bearing amphibolites from the Angurep metamorphic complex in the terrigenous mélange unit was quarried in the right bank of the Shalap River. The block has a size of more than 100 m. The rocks are represented by garnet amphibolites (samples 19-261, 19-262), medium- and fine-grained, dark-green massive or indistinctly banded (Fig. 4). Garnet content varies along the cross-section, from zero or single grains to 15 %. At the eastern edge of the quarry, the amphibolites are intersected by a yellowish-gray fine-grained mica-quartz vein, presumably produced by regressive metamorphism of the granitoid vein (sample 19-263). Northwest of the Shalap mélange area, near Kytmanovo Village, the quarry penetrated the mélange area of the same name, represented by lens-shaped blocks of limestones and green-stone basalts of the Alambay formation (see Fig. 1, sample 20-331,) in the matrix of schistose greywacke and serpentine schists. The basalts contain numerous calcite veinlets and segregations.

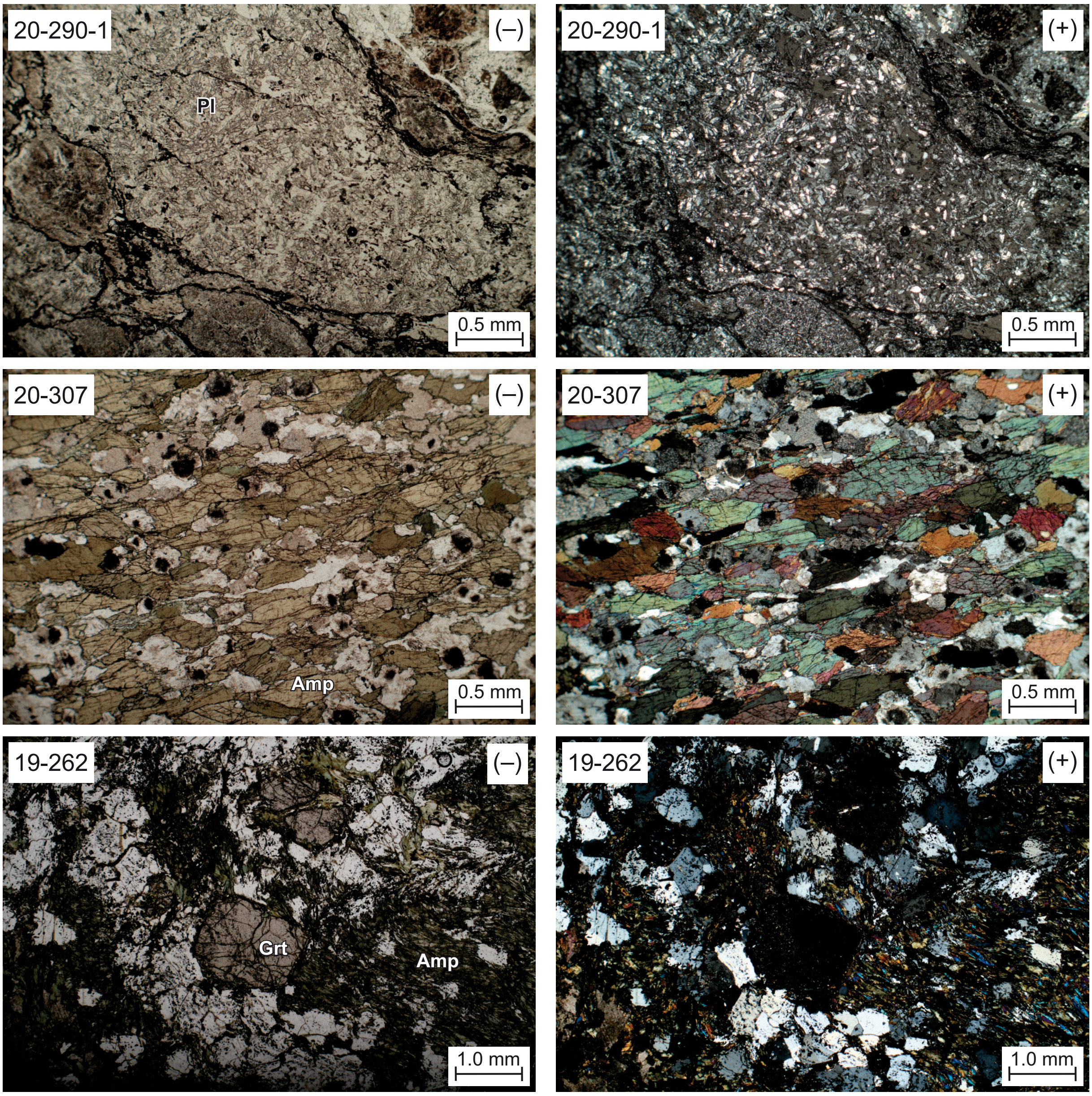

Fig. 4. Micrographs of thin sections of the studied rocks in parallel and crossed nicols.
Sample 20-290-1 – brecciated aphyric basalts from serpentinite mélange; sample 20-307 – amphibolites of the Angurep complex, here are first-generation greenish-brown hornblende and saussuritized plagioclase; sample 19-262 – garnet amphibolites in Shalap mélange. Pl – plagioclase, Amp – amphibole, Grt – garnet.

Metamorphic rocks of the Angurep complex were quarried near Popovichi Village along the Angurep and Anamas rivers (samples 20-307, 20-311, 20-313, 20-322). The AOZ gabbro and dolerite samples (19-241, 19-243, 19-243-1) were taken from the Tyagun-Alambay area of the AOZ. The data on composition of the rock samples and their sampling sites are presented in App. 1, Table 1.1 and in Fig. 1 and 2.

5. METHODS

Contents of petrogenic elements in the rocks were determined by X-ray fluorescence analysis, and those of rare and rare-earth elements – by the ICP-MS method using Shared Research Facilities of Multi-Element and Isotope Researches of SB RAS (Novosibirsk). The major task of petrochemical and geochemical analyses was to extract typical features of photoliths which yielded amphibolites. This involved the elements immobile in metamorphism (Ti, Y, Zr, Nb, REE). The sampling did not include migmatized varieties which were mismatched with the original composition of protoliths. The muscovite age was determined by the $^{40}Ar/^{39}Ar$ step-heating for mineral fractions, after [Travin, 2016].

6. GEOCHEMICAL COMPOSITION OF ROCKS

Based on the original data, consideration was given to the petrochemical and geochemical features of metabasalt and amphibolite samples from tectonic blocks in the

Shalap ophiolite mélange, and a comparative compositional analysis was made on gabbro and dolerites of the Togul-Sungai ophiolite mélange area (App. 1, Table 1.2).

Some of the selected basite samples are significantly transformed by secondary processes as reflected in high loss on ignition. Their geochemical features were extracted based on the data on rare elements; since the rocks studied were involved in metasomatic and metamorphic transformations, use has been made of the diagrams with low-mobility elements (Th, Nb, Ti, V) proposed to interpret ophiolites in different geodynamic settings [Pearce, 2008, 2014].

The studied samples are partially transformed by low-temperature metamorphic processes; in particular, basalt sample 20-331 contains the calcite veins which leads to high loss on ignition (7.1 wt. %). According to total alkalinity, metabasalts belong to subalkaline series and have high titanium (more than 2 wt. %) and magnesium (9.5–11.1 wt. %) contents. Amphibolites have 43 to 56 % silica content and belong to the rocks of normal, less often moderate alkalinity; unlike the metabasalts, the amphibolites of the Angurep complex are characterized by low TiO_2 content ranging from 0.13 to 1.76 wt. %. There are distinguished two groups of amphibolites – with moderate (1.6–1.8 wt. %) and low (less than 0.8 wt. %) content of TiO_2. On Zr/Ti–Nb/Y diagram for low-mobility highly charged elements, imaging points for amphibolite composition fall within the basalt field and are comparable to those for composition of gabbro from the tectonic slab contacting with apodunite serpentinites of the Togul-Sungai massif in the west. These data allow the protoliths of amphibolites to be assigned to tholeitic basalts of normal alkalinity. Unlike those, the metabasalts have high Nb/Y contents and fall within the alkaline basalt field (Fig. 5, a).

The geodynamic setting of the formation of ophiolites can be judged from the data on Nb/Y-Zr/Y diagram [Condie, 2005]. Composition points of the amphibolites and gabbro considered lie in the area of magmatic systems unaffected by the plume source (NPS) in the mid-ocean ridge basalt field and are close to the data on the Woodlark back-arc

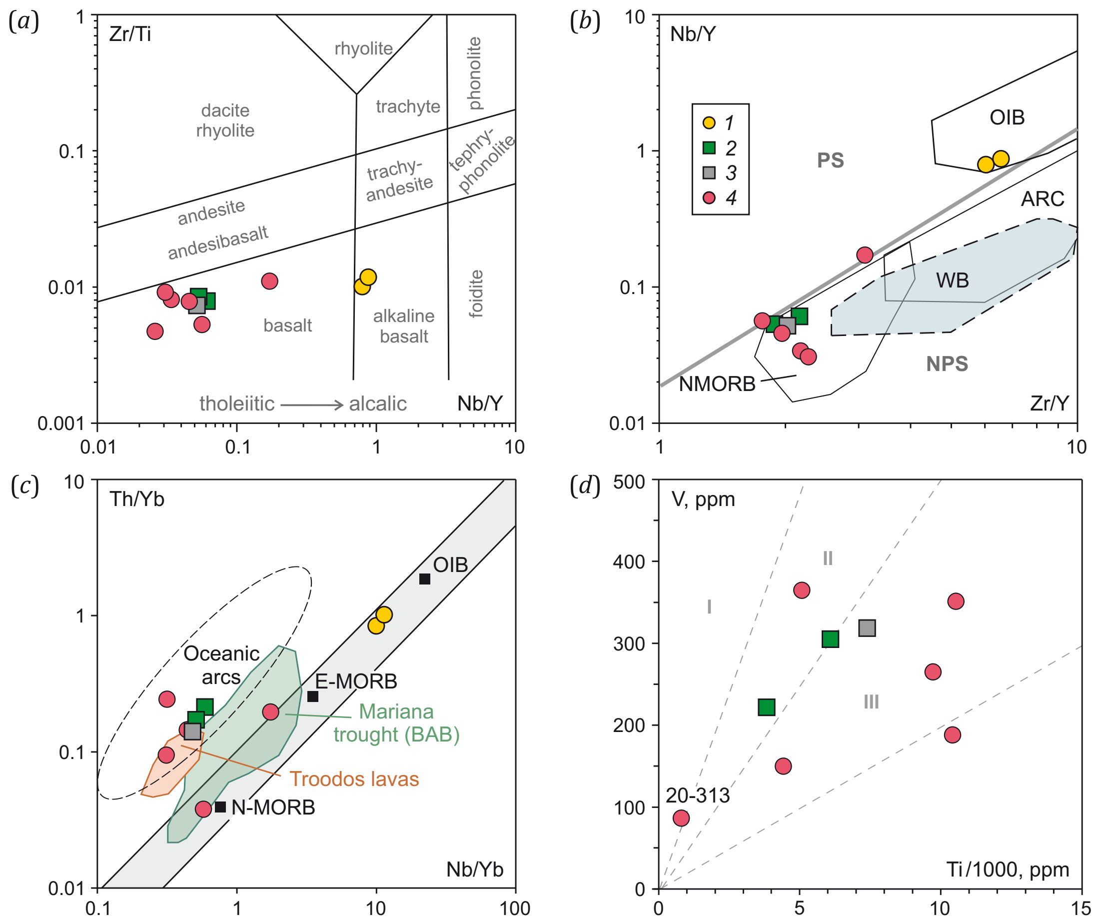

Fig. 5. Variation diagrams: (*a*) – Zr/Ti – Nb/Y [Pearce, 2014]; (*b*) – Nb/Y – Zr/Y [Condie, 2005]; (*c*) – Th/Yb – Nb/Yb [Pearce, 2008, 2014]; (*d*) – V – Ti [Shervais, 1982] with a range of compositions of various types of rocks identified in [Pearce, 2014].
1 – metabasalts, *2* – gabbro, *3* – dolerite (19-243-1), *4* – amphibolites. Fields of rocks: NMORB – normal mid-ocean ridge basalts, OIB – intraplate oceanic island basalts, ARC – island-arc basalts [Condie, 2005]; WB – basalts of the Woodlark Basin (Pacific Ocean) after [Dril et al., 1997]; Oceanic arcs – island-arc basalts of intraoceanic arcs; Troodos lavas – Troodos ophiolite lavas [Pearce, 2014]; Mariana trough (BAB) – back-arc basalts of the Mariana Trough [Pearce, 2008]; areas of rocks with a plume (PS) and without a plume (NPS) source [Condie, 2005], I – boninites, II – basalts of proximal island arcs and back-arc basins, III – distal island-arc, back-arc basin and MORB basalts [Pearce, 2014].

basin. The metabasalts, on the contrary, are plume-related OIB – intraplate ocean island basalts (Fig. 5, b). On Nb/Yb-Th/Yb diagram, used to interpret ophiolite complexes [Pearce, 2008, 2014], the metabasalts have high Nb/Yb and Th/Yb ratios and lie in the composition field of basalts unrelated to subduction zones, between E-MORB – OIB points (Fig. 5, c), whereas the amphibolite points lie higher than this field of basalts whose formation was influenced by subduction processes – they lie in the field of intra-oceanic island arc basalts, being associated with the data on the back-arc basalts of the Mariana trough and the Late Mesozoic supra-subduction zone-related Troodos ophiolitic lavas [Pearce et al., 1984]. The imaging points for amphiboilite composition are widely scattered over Ti – V diagram and geochemically comparable to proximal island-arc tholeites and distal back-arc basin and N-MORB basalts (Fig. 5, d).

The distribution of rare-earth elements shows that metabasalt spectra have a negative slope (with a predominance of light lantanoids) and are most close to oceanic island basalt plots (Fig. 6, a). The distribution plots of immobile elements normalized to N-MORB also show their belonging to the rocks from the enriched mantle source similar to oceanic-island or E-MORB basalts (Fig. 6, b). The distribution plots of chondrite-normalized rare-earth elements in garnet amphibolites of the Shalap ophiolite mélange have a subhorizontal spectrum or a shallow negative slope (Fig. 6, c). This can be attributed to island-arc tholeite basalts (IATB) and back-arc basin basalts (BABB). Compared to them, the rare-earth spectra in the amphibolites of the Angurep tectonic slab have lower REE contents and coincide with the BABB spectra. According to the distribution of immobile elements, the amphibolites of the Angurep complex form a compact field with a Th-, Nb-, Hf- and Ti-element content, similar to that plotted for the supra-subduction zone-related ophiolites, and indicate the amphibolite formation either near the island arc or in the back-arc basin (Fig. 6, d).

The rare-earth spectra of the gabbro and dolerite samples from the Togul-Sungai massif are identical to the spectra of the amphibolites of the Angurep complex and typical for melts from supra-subduction zones. Amphibolite sample 20-313 has the lowest rare-element content which testifies to the fact that it was derived from the source more depleted than the MORB mantle; its protolith may be a metamorphosed cumulative rock. This sample is characterized by the highest Al_2O_3 and CaO contents and a low TiO_2 content (0.13 %), not typical of mafic volcanic rocks.

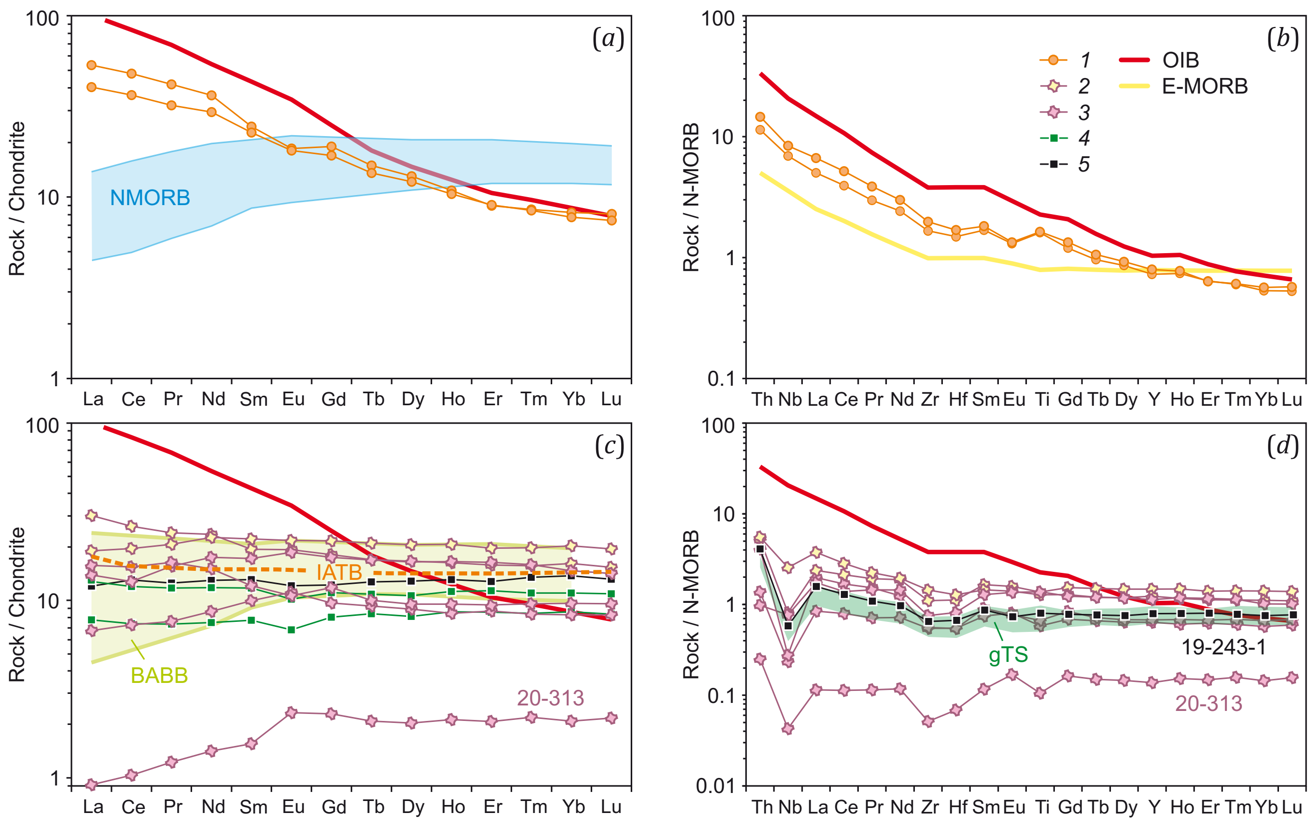

Fig. 6. Distribution of rare-earth (*a*, *b*) and low-mobility elements (*c*, *d*) in the rocks of the Alambay ophiolite zone.
1 – metabasalts in the Shalap mélange; *2* – garnet amphibolites in the Shalap mélange area; *3* – amphibolites of the Angurep tectonic slab; *4* – gabbro of the Togul-Sungai ultrabasite massif; *5* – dolerite (sample 19-243-1). Fields: NMORB – normal mid-ocean ridge basalts, BABB – back-arc basin basalts, gTS – gabbro of the Togul-Sungai massif. Lines: IATB – upper boundary of the island-arc tholeiitic basalt field, OIB – ocean island basalts, E-MORB – enriched mid-ocean ridge basalts. The diagram is drawn up based on the original data and the data from [Sharaskin, 1992; Simonov et al., 1999; Sun, McDonough, 1989]. The element values are normalized to the C1 chondrite composition [Boynton, 1984] and to the N-MORB composition [Sun, McDonough, 1989].

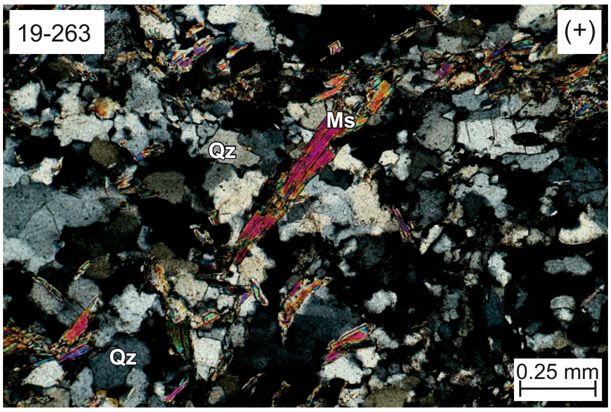

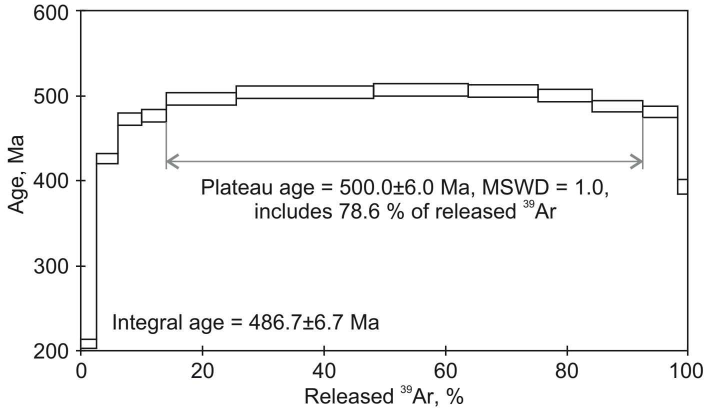

Fig. 7. Micrograph of muscovite-quartz apogranite rock (sample 19-263) and argon-argon age spectrum of muscovite.

According to their geochemical composition, the basalts, occurring as blocks in the Shalap mélange, were plume-derived and may be the fragments of oceanic islands (OIB). Geochemical features of gabbro of the Togul-Sungai ophiolite massif imply that it is supra-subduction zone-related. The basites that served as the protoliths for amphibolites were produced by melting out of a similar magmatic source, in the paleogeodynamic setting of oceanic island arc.

7. ARGON-ARGON DATING

The argon-argon dating was performed on muscovite from the mica-quartz apogranite vein intersecting the garnet amphibolite block in terrigenous facies of the Shalap mélange. Muscovite has differently oriented occurrence patterns, without deformational structures, and represents the latest post-tectonic mineral formed in granitoid veins at the stage of low-temperature diaphthoresis of the terrigenous mélange rocks. The argon-argon age of muscovite determined using the plateau method (App. 1, Table 1.3; Fig. 7) is 500.0±6 Ma and can be considered as the upper time limit for the completion of retrograde metamorphic evolution in the complex.

8. RESULTS AND DISCUSSION

As a result of research in serpentinite mélange of the Shalap area of the AOZ, there were found basalt blocks with petrogeochemical characteristics of ocean island basalts (TiO_2=2.0 %, P_2O_5=0.22 %, Nb=16 ppm, Zr/Nb=7.6, La/Yb_n= =5.54). The metamorphic rocks, represented by garnet-bearing and non-garnet amphibolites of the Angurep complex, compose a narrow tectonic slab, lying between the island-arc acid effusive rock slab and the olistostrome unit, and the blocks in the terrigenous facies of the Shalap mélange. In the mélange, there is a superimposition of rock blocks comprising large tectonic slabs which lie on both sides of the AOZ; these are metabasalts of the Alambay formation, microquartzites, including manganiferous, comprising the Kivdinskaya tectonic slab, amphibolites of the Angurep complex, and limestones of the Gavrilov formation. The tectonic slab package as a whole can be considered as an accretionary complex, and the Shalap mélange area – as an axial part of the structure corresponding to the paleosubduction zone. Amphibolites of the AOZ correspond in their petrogeochemical features to the island-arc tholeitic basalts and contrast sharply with intraplate basalts including the basalts of the Alambay formation. This is thought to be a feature by which the rocks of the Angurep complex differ from most of the subductional metamorphites of the ASFA, characterized by the presence of metabasites with a chemical composition corresponding to intraplate basalts [Volkova, Sklyarov, 2007]. If further studies confirm the island-arc nature of the protolith of amphibolites of the Angurep complex, it will then be possible to talk about tectonic erosion of basalt basement of the Early Cambrian island arc [Safonova, Perfilova, 2022], changed to the episode of exhumation of the island-arc metabasite slab. The ideas of the existence of tectonic erosion in the Early Cambrian Salair subduction zone allow resolving one of the geological contradictions in the region: most of the Lower Cambrian Salair volcanic sections are composed of acid and intermediate rocks (Pecherkino formation and its analogs), not typical of the oceanic island arcs. During tectonic erosion, the basalt basement of the oceanic island arc could be largely subducted. The fact that the AOZ is the northern continuation of the Katun accretionary complex of the Altai Mountains [Dobretsov et al., 2004; Shokalskii et al., 2000] suggests the subducted terrigenous and serpentinite mélanges were both formed and exhumed during the transformation of the subduction zone as a result of collision between the oceanic island and island arc and the subsequent reformation of the island-arc system. The Lower Cambrian marmorized limestone blocks in mélange can be the fragments of carbonate sedimentary cover of the oceanic island. The Vendian–Early Cambrian and Late Cambrian–Ordovician Salair island-arc volcanic stages, separated by the late Lower and Middle Cambrian amagmatic periods of carbonate and terrigenous deposition (Suenga and Kinterep formations) and a large structural unconformity [State Geological Map..., 2015; Shokalskii et al., 2000; Vetrova et al., 2022], are in good agreement with this model. The Vendian–Lower Cambrian Salair island-arc volcanites could be the protolith of garnet amphibolites of the Angurep complex.

The detailed geochronological studies of subduction metamoirphites of the Angurep complex are the challenges of the future; the present-day peak metamorphism can be estimated approximately at ~520 Ma, or at somewhat earlier date, considering that the closure of amphibole isotopic system occurred after some rock cooling from metamorphic peak conditions. By 500 Ma, the rocks were brought to the upper crustal depths. The 520–500 Ma interval corresponds to the time of collision of the island-arc system with oceanic islands and to the Salair Pacific-type orogeny.

9. CONCLUSIONS

As a result of the research, the authors made the following conclusions.

1. In the Shalap mélange, there are basalt blocks of the Alambay formation with petrogeochemical features corresponding to oceanic island basalts (OIB).

2. Metamorphic rocks of the Angurep complex, represented by garnet-bearing and non-garnet amphibolites, compose a tectonic slab incorporated into the imbricated accretionary complex. Metamorphic rocks also comprise blocks in polymictic facies of the Shalap mélange. Amphibolites of the Angurep complex are similar in their petrogeochemical features to intracontinental island-arc tholeitic basalts and identical to gabbroids from basite-hyperbasite complexes of the Alambay ophiolite zone.

3. The Shalap mélange is a fragment of the Cambrian Salair paleosubduction zone. The mélange complex formation is related to the Early Cambrian island-arc collision with oceanic islands. The processes of subduction and exhumation in this paleosubduction zone stopped around 500 Ma.

10. ACKNOWLEDGEMENTS

The authors express their gratitude to I.S. Novikov, Dr. Sc. (Geol.-Min.), and N.S. Tychkov, Cand. Sc. (Geol.-Min.), for assistance in conducting fieldwork, to S.A. Kargapolov, Cand. Sc. (Geol.-Min.), and V.N. Tokarev, Cand. Sc. (Geol.-Min.), for the consult on Salair geology, to E.S. Zhimuleva, Cand. Sc. (Tech.), for help in preparing manuscript, and to V.A. Belyaev, Cand. Sc. (Geol.-Min.), and the anonymous reviewer for the revision notes.

11. CONTRIBUTION OF THE AUTHORS

All authors made an equivalent contribution to this article, read and approved the final manuscript.

12. DISCLOSURE

The authors declare that they have no conflicts of interest relevant to this manuscript.

13. REFERENCES

Boynton W.V., 1984. Cosmochemistry of the Rare Earth Elements: Meteorite Studies. Developments in Geochemistry 2, 63–114. https://doi.org/10.1016/B978-0-444-42148-7.50008-3.

Condie K.C., 2005. High Field Strength Element Ratios in Archean Basalts: A Window to Evolving Sources of Mantle Plumes? Lithos 79 (3–4), 491–504. https://doi.org/10.1016/j.lithos.2004.09.014.

Dobretsov N.L., Buslov M.M., Yu U., 2004. Fragments of Oceanic Islands in Accretion-Collision Areas of Gorny Altai and Salair, Southern Siberia, Russia: Early Stages of Continental Crustal Growth of the Siberian Continent in Vendian – Early Cambrian Time. Journal of Asian Earth Sciences 23 (5), 673–690. https://doi.org/10.1016/S1367-9120(03)00132-9.

Dril S.I., Kuzmin M.I., Tsipukova S.S., Zonenshain L.P., 1997. Geochemistry of Basalts from the Western Woodlark, Lau and Manus Basins: Implications for Their Petrogenesis and Source Rock Compositions. Marine Geology 142 (1–4), 57–83. https://doi.org/10.1016/S0025-3227(97)00041-8.

Festa A., Pini G.A., Dilek Y., Codegone G., 2010. Mélanges and Mélange-Forming Processes: A Historical Overview and New Concepts. International Geology Review 52 (10–12), 1040–1105. https://doi.org/10.1080/00206810903557704.

Konovalova O.G., Prusevich N.A., 1977. Dunite-Harzburgite Massifs of the Kuznetsk Alatau and Salair (Geological Features, Formation Conditions, Chromite Content). Nauka, Novosibirsk, 166 p. (in Russian) [Коновалова О.Г., Прусевич Н.А. Дунит-гарцбургитовые массивы Кузнецкого Алатау и Салаира (Геологические особенности, условия формирования, хромитоносность). Новосибирск: Наука, 1977. 166 с.].

Pearce J.A., 2008. Geochemical Fingerprinting of Oceanic Basalts with Applications to Ophiolite Classification and the Search for Archean Oceanic Crust. Lithos 100 (1–4), 14–48. https://doi.org/10.1016/j.lithos.2007.06.016.

Pearce J.A., 2014. Immobile Element Fingerprinting of Ophiolites. Elements 10 (2), 101–108. https://doi.org/10.2113/gselements.10.2.101.

Pearce J.A, Harris N.B.W., Tindle A.G., 1984. Trace Element Discrimination Diagrams for the Tectonic Interpretation of Granitic Rocks. Journal of Petrology 25 (4), 956–983. https://doi.org/10.1093/petrology/25.4.956.

Pinus G.V., Kuznetsov V.A., Volokhov I.M., 1958. Hyperbasites of the Altai-Sayan Folded Area. Gosgeoltekhizdat, Moscow, 295 p. (in Russian) [Пинус Г.В., Кузнецов В.А., Волохов И.М. Гипербазиты Алтае-Саянской складчатой области. М.: Госгеолтехиздат, 1958. 295 с.].

Raymond L.A., 2019. Origin of Melanges of the Franciscan Complex, Diablo Range and Northern California: An Analysis and Review. Geosciences 9 (8), 338. https://doi.org/10.3390/geosciences9080338.

Safonova I., Perfilova A., 2022. Survived and Disappeared Intra-Oceanic Arcs of the Paleo-Asian Ocean: Evidence from Kazakhstan. National Science Review 10 (2), nwac215. https://doi.org/10.1093/nsr/nwac215.

Sharaskin A.Ya., 1992. Tectonics and Magmatism of the Marginal Seas in Connection with the Problems of the Evolution of the Crust and Mantle. Nauka, Moscow, 163 p. (in Russian) [Шараськин А.Я. Тектоника и магматизм окраинных морей в связи с проблемами эволюции коры и мантии. М.: Наука, 1992. 163 с.].

Shervais J.W., 1982. Ti–V Plots and the Petrogenesis of Modern and Ophiolitic Lavas. Earth and Planetary Science

Letters 59 (1), 101–118. https://doi.org/10.1016/0012-821X(82)90120-0.

Shokalskii S.P., Babin G.A., Vladimirov A.G., Borisov S.M., Gusev N.I., Tokarev V.N., Zybin V.A., Dubskii V.S. et al., 2000. Correlation of Igneous and Metamorphic Complexes of the Western Part of the Altai-Sayan Folded Region. GEO, Novosibirsk, 188 p. (in Russian) [Шокальский С.П., Бабин Г.А., Владимиров А.Г., Борисов С.М., Гусев Н.И., Токарев В.Н., Зыбин В.А., Дубский В.С. и др. Корреляция магматических и метаморфических комплексов западной части Алтае-Саянской складчатой области. Новосибирск: Гео, 2000. 188 с.].

Simonov V.A., Kolobov V.Yu., Peive A.A., 1999. Petrology and Geochemistry of Geodynamic Processes in Central Atlantic. Publishing House of SPC UIGGM SB RAS, Novosibirsk, 224 p. (in Russian) [Симонов В.А., Колобов В.Ю., Пейве А.А. Петрология и геохимия геодинамических процессов в Центральной Атлантике. Новосибирск: Изд-во НИЦ ОИГГМ СО РАН, 1999. 224 с.].

State Geological Map of the Russian Federation, 2007. Altai-Sayansk Series. Scale 1:1000000. Sheet N-45 (Novokuznetsk). Explanatory Note. VSEGEI, Saint Petersburg, 665 p. (in Russian) [Государственная геологическая карта Российской Федерации. Серия Алтае-Саянская. Масштаб 1:1000000. Лист N-45 (Новокузнецк): Объяснительная записка. СПб.: ВСЕГЕИ, 2007. 665 с.].

State Geological Map of the Russian Federation, 2015. Kuzbass Series. Scale 1:200000. Sheet N-45-XIII (Maslyanino). Explanatory Note. Moscow Branch of VSEGEI, Moscow, 276 p. (in Russian) [Государственная геологическая карта Российской Федерации. Серия Кузбасская. Масштаб 1:200000. Лист N-45-XIII (Маслянино): Объяснительная записка. М.: МФ ВСЕГЕИ, 2015. 276 с.].

State Geological Map of the Russian Federation, 2019. Kuzbass Series. Scale 1:200000. Sheet N-45-XXVI (Tselinnoye). Explanatory Note. Moscow Branch of VSEGEI, Moscow, 89 p. (in Russian) [Государственная геологическая карта Российской Федерации. Серия Кузбасская. Масштаб 1:200000. Лист N-45-XXVI (Целинное): Объяснительная записка. М.: МФ ВСЕГЕИ, 2019. 89 с.].

Sun S.-S., McDonough W.F., 1989. Chemical and Isotopic Systematics of Oceanic Basalts: Implications for Mantle Composition and Processes. Geological Society of London Special Publications 42 (1), 313–345. https://doi.org/10.1144/GSL.SP.1989.042.01.19.

Travin A.V., 2016. Thermochronology of Early Paleozoic Collisional and Subduction-Collisional Structures of Central Asia. Russian Geology and Geophysics 57 (3), 434–450. https://doi.org/10.1016/j.rgg.2016.03.006.

Vetrova N.I., Vetrov E.V., Letnikova E.F., Soloshenko N.G., 2022. Age of the Kinterep Formation of the Northwestern Salair: Chemostratigraphy and U-Pb Zircon Dating. Geodynamics & Tectonophysics 13 (2), 0597 (in Russian) [Ветрова Н.И., Ветров Е.В., Летникова Е.Ф., Солошенко Н.Г., 2022. Возраст кинтерепской свиты Северо-западного Салаира: данные хемостратиграфии и U-Pb датирования циркона. Геодинамика и тектонофизика. Т. 13. № 2. 0597]. https://doi.org/10.5800/GT-2022-13-2s-0597.

Vladimirov A.G., Gibsher A.S., Esin S.V., Izoh A.E., Kargopolov S.A., Kruk N.N., Malikova O.Yu., Plotnikov A.V. et al., 1994. Petrological and Geochronological Study of Igneous and Metamorphic Complexes of the Western Part of the Altai-Sayan Folded Region. Interim Report on the Project. 403 p. (in Russian) [Владимиров А.Г., Гибшер А.С., Есин С.В., Изох А.Э., Каргополов С.А., Крук Н.Н., Маликова О.Ю., Плотников А.В. и др. Петролого-геохронологическое исследование магматических и метаморфических комплексов западной части Алтае-Саянской складчатой области: Промежуточный отчет по проекту. 1994. 403 с.].

Volkova N.I., Sklyarov E.V., 2007. High-Pressure Complexes of Central Asian Fold Belt: Geologic Setting, Geochemistry, and Geodynamic Implications. Russian Geology and Geophysics 48 (1), 83–90. https://doi.org/10.1016/j.rgg.2006.12.008.

Zhimulev F.I., Kargopolov S.A., Travin A.V., Proshenkin A.I., Letnikova E.F., Stepanov A.S., Novikov I.S., Vetrov E.V., Dokashenko S.A., Gillespi D., 2020. History of the Geological Development of the Salair Folded Zone, New Data on Metamorphism and the Age of Magmatic Activity. In: Fundamental Problems of Tectonics and Geodynamics. Proceedings of LII Tectonic Meeting (January 28 – February 01, 2020). Vol. 1. GEOS, Moscow, p. 219–223 (in Russian) [Жимулев Ф.И., Каргополов С.А., Травин А.В., Прошенкин А.И., Летникова Е.Ф., Степанов А.С., Новиков И.С., Ветров Е.В., Докашенко С.А., Гиллеспи Д. История геологического развития Салаирской складчатой зоны, новые данные о метаморфизме и возрасте магматической активности // Фундаментальные проблемы тектоники и геодинамики: Материалы LII тектонического совещания (28 января – 01 февраля 2020 г.). М.: ГЕОС, 2020. Т. 1. С. 219–223].

Zhimulev F.I., Pospeeva E.V., Potapov V.V., Novikov I.S., Kotlyarov A.V., 2023. Salair–Gornaya Shoria Junction (Northwestern Central Asian Orogenic Belt): Deep Structure and Tectonics from Magnetotelluric Data. Russian Geology and Geophysics 64 (5), 558–570. https://doi.org/10.2113/RGG20224479.

APPENDIX 1

Table 1.1. Coordinates of sampling sites and geological position of the selected samples

№	Coordinates of sampling site	Rock	Geological position
20-290-1	53°6'16.62" 85°39'31.74"	Greenstone basalts	Block in serpentinite mélange. Shalap mélange area
20-331	53°28'13.40" 85°27'51.94"	Greenstone basalts	Block in serpentinite mélange. Kytmanovo mélange area
19-261	53° 5'17.63" 85°50'20.18"	Garnet amphibolites	A block of metamorphites from the Angurep complex in terrigenous facies of the Shalap mélange
19-262	53° 5'17.39" 85°50'22.17"	Garnet amphibolites	A block of metamorphites from the Angurep complex in terrigenous facies of the Shalap mélange
20-307	53° 2'49.38" 86°10'25.22"	Garnet amphibolites, banded, migmatized	Angurep metamorphic complex
20-311	53° 0'48.78" 86°14'37.90"	Coarse-grained amphibolites	Angurep metamorphic complex
20-313	53° 0'41.29" 86°16'41.62"	Coarse- and giant-grained amphibolites, pegmatoid, chloritized	Angurep metamorphic complex
20-322	53° 0'12.61" 86°15'46.28"	Chloritized amphibolites	Angurep metamorphic complex
19-263	53° 5'17.13" 85°50'23.51"	Muscovitized microgranites	A block of metamorphites from the Angurep complex in terrigenous facies of the Shalap mélange
19-240-1	53°57'14.42" 85°46'52.95"	Gabbro	Segregated serpentinite bodies in the Togul-Sungai massif of the AOZ Tyagun-Alambay area
19-243	53°56'16.47" 85°47'29.76"	Gabbro	Segregated serpentinite bodies in the Togul-Sungai massif
19-243-1	53°56'16.47" 85°47'29.76"	Dolerites	The dike intersecting the gabbro block in serpentinites of the Togul-Sungai massif

Table 1.2. Chemical composition of the rocks of the Shalap mélange and the Angurep metamorphic complex

Rocks	Greenstone basalts		Amphibolites						Ms-Qz rock
Compo-nents	20-290-1	20-331	20-307	20-311	20-313	20-322	19-261	19-262	19-263
SiO_2, wt. %	47.25	43.23	48.65	48.33	44.89	49.80	55.85	45.99	73.58
TiO_2	2.03	2.07	1.76	0.74	0.13	0.85	1.74	1.62	0.31
Al_2O_3	11.22	12.91	15.17	17.54	19.47	14.07	13.44	13.20	12.38
Fe_2O_3*	11.23	12.10	14.67	7.74	6.17	13.84	14.32	13.48	3.82
MnO	0.15	0.21	0.22	0.13	0.10	0.18	0.28	0.31	0.05
MgO	11.05	9.49	6.12	6.74	9.35	4.27	2.68	4.73	1.68
CaO	9.02	8.32	7.93	13.18	15.39	8.31	6.17	11.16	0.58
Na_2O	1.79	2.75	3.26	2.55	0.80	1.71	3.94	3.18	2.49
K_2O	1.80	1.10	0.97	0.47	0.20	0.05	0.24	0.19	1.48
P_2O_5	0.22	0.27	0.15	0.09	0.02	0.11	0.29	0.23	0.06
BaO	0.12	0.05	0.03	0.01	0.01	<0.01	0.01	0.01	0.05
SO_3	0.07	<0.03	<0.03	<0.03	<0.03	0.07	<0.03	0.12	<0.03
V_2O_5	0.04	0.04	0.06	0.03	0.02	0.07	0.03	0.05	0.01
Cr_2O_3	0.04	0.06	0.01	0.02	0.01	<0.01	<0.01	0.01	<0.01
NiO	<0.01	0.02	<0.01	<0.01	<0.01	<0.01	<0.01	<0.01	0.01
LOI	3.72	7.06	1.14	2.39	2.66	6.41	0.66	5.88	2.74
Total	99.77	99.73	100.16	99.98	99.24	99.74	99.69	100.16	99.26
Rb, g/t	28	15.6	15.7	6.3	3.4	0.94	2.3	1.84	24
Sr	306	268	238	309	239	229	126	117	99
Y	20	22	32	17.8	3.9	18.9	42	35	15.6
Zr	123	146	56	40	3.8	41	82	107	147
Nb	16.1	19.5	1.79	0.55	0.10	0.64	1.90	5.9	22
Cs	1.26	0.57	0.20	<0.1	0.10	0.10	<0.1	0.13	0.30
Ba	933	379	197	86	32	17.6	93	36	360
La	12.5	16.6	4.4	2.1	0.29	4.9	6.0	9.4	36
Ce	29	39	10.4	6.0	0.85	12.6	16.0	21	55
Pr	3.9	5.1	1.92	0.94	0.15	2.0	2.6	3.0	8.5
Nd	17.7	22	10.6	5.2	0.86	9.1	13.7	14.2	32
Sm	4.4	4.8	3.4	1.96	0.31	2.4	4.4	3.8	5.7
Eu	1.33	1.36	1.39	0.82	0.17	0.79	1.61	1.43	1.21
Gd	4.4	4.9	4.6	2.5	0.60	3.1	5.7	4.7	4.1
Tb	0.64	0.71	0.81	0.44	0.10	0.48	1.01	0.81	0.60
Dy	3.9	4.2	5.4	2.9	0.66	3.1	6.7	5.4	3.1
Ho	0.75	0.78	1.20	0.61	0.15	0.69	1.50	1.18	0.62
Er	1.90	1.88	3.5	1.85	0.44	2.0	4.2	3.4	1.78
Tm	0.27	0.28	0.52	0.27	0.072	0.31	0.64	0.51	0.28
Yb	1.62	1.72	3.1	1.75	0.44	2.0	4.3	3.4	1.90
Lu	0.24	0.26	0.46	0.27	0.071	0.31	0.63	0.50	0.29
Hf	3.0	3.5	1.68	1.12	0.14	1.12	2.3	2.6	3.4
Ta	1.06	1.26	0.072	0.27	<0.05	<0.05	0.19	0.45	1.61
Th	1.37	1.75	0.12	0.17	<0.03	0.49	0.62	0.67	3.1
U	0.33	0.49	0.39	0.11	<0.02	0.52	0.53	0.15	0.68

Note. * – total iron is presented as Fe_2O_3.

Table 1.3. $^{40}Ar/^{39}Ar$ dating results

T (°C)	t (min)	^{40}Ar (STP), $\times10^{-9}$	$^{40}Ar/^{39}Ar$	±1σ	$^{38}Ar/^{39}Ar$, $\times10^{-2}$	±1σ, $\times10^{-3}$	$^{37}Ar/^{39}Ar$, $\times10^{-2}$	±1σ, $\times10^{-3}$	$^{36}Ar/^{39}Ar$, $\times10^{-2}$	±1σ, $\times10^{-3}$	Ca/K	$\sum^{39}Ar$ (%)	Age (Ma) ±1σ	±1σ
Mica 19-263, weight quantity 41.98 mg, J=0.006025±0.000095; integral age = 486.7±6.7 Ma; plateau age (750–1130 °C)=16.8±0.4 Ma														
500	10	75.5	38.711	0.133	2.488	2.38	11.81	18.3	6.221	1.48	0.43	2.5	208.4	5.3
600	10	148.1	53.527	0.078	1.668	1.46	20.02	12.4	3.162	0.64	0.72	6.1	425.8	6.2
675	10	166.2	55.496	0.124	1.72	0.65	6.9	7.6	1.98	1.04	0.25	10.1	472.1	7.1
730	10	169.4	56.208	0.050	1.756	1.02	2.21	7.2	2.052	1.06	0.08	14.0	476.3	7.1
800	10	499.0	56.151	0.100	1.308	0.08	2.36	6.1	1.221	0.64	0.08	25.6	496.2	7.1
870	10	967.8	55.757	0.094	1.173	0.58	1.28	4.7	0.759	0.36	0.05	48.2	504.2	7.0
920	10	674.9	56.264	0.073	1.121	0.8	0.61	4.7	0.829	0.53	0.02	63.8	506.7	7.1
970	10	497.8	57.075	0.065	1.082	0.87	0.14	10.7	1.18	0.87	0.00	75.2	504.8	7.3
1020	10	418.1	60.675	0.069	1.59	1.61	2.0	16.9	2.583	1.12	0.07	84.2	500.3	7.4
1090	10	367.6	57.292	0.131	1.881	1.25	3.6	18.2	1.961	0.9	0.13	92.5	487.5	7.2
1170	10	261.9	59.614	0.162	1.27	2.01	6.38	29.1	3.027	0.63	0.23	98.3	480.7	6.9
1250	10	85.3	64.346	0.368	2.359	3.21	7.06	32.1	8.11	2.7	0.25	100.0	392.9	9.1

Note. J – a parameter characterizing the magnitude of neutron flux.